STEM CELLS AND DEVELOPMENT
Volume 22, Number 7, 2013

DOI: 10.1089/scd.2012.0583



# Adult Neurogenesis in the Crayfish Brain: The Hematopoietic Anterior Proliferation Center Has Direct Access to the Brain and Stem Cell Niche

Paula Grazielle Chaves da Silva,[1,2] Jeanne L. Benton,[1] David C. Sandeman,[1] and Barbara S. Beltz[1]

Neuronal stem cells residing in a niche on the surface of the adult crayfish (*Procambarus clarkii*) brain are not self-renewing. However, the neuronal precursors in the niche are not depleted despite continued neurogenesis and the exit of precursor cells from the niche throughout the organism's life. The neurogenic niche is therefore not a closed system, and we have previously proposed that the stem cell pool is replenished from the hematopoietic system. Noonin et al. (2012) demonstrated that the hematopoietic system in the crayfish *Pacifastacus leniusculus* includes an anterior proliferation center (APC) lying near the brain; they suggest that multipotent stem cells are concentrated in this region, and that the APC may provide neuronal stem cells for adult neurogenesis. The present study extends this work by describing the location and cellular organization of hematopoietic tissues in *P. clarkii.* We find that the APC lies within the cor frontale, or auxiliary heart, which pumps hemolymph to the brain and eyes through the cerebral and ophthalmic arteries, respectively. Vascular extensions of the cerebral artery converge on the neurogenic niche. APC cells lie in layered sheets within the cor frontale and form rosette-like structures reminiscent of stem cells in other developing tissues. We confirm here that APC cells in *P. clarkii* have characteristics of multipotent stem cells, and that their location within the cor frontale allows direct access to regions in the central nervous system in which adult neurogenesis occurs.

## Introduction

### *Adult neurogenesis in crayfish*

As in many vertebrate and invertebrate species, new neurons are born and integrated into circuits in the brains of adult decapod crustaceans [1,2]. In the crayfish, *Procambarus clarkii*, the precursor cell lineage producing the adult-born neurons has been identified beginning with the first-generation progenitors (stem cells) located in a niche on the ventral surface of the brain [3,4]. Experiments have shown that these first-generation precursors divide geometrically, symmetrically, and that both daughters migrate away from the niche, traveling in streams to proliferation zones associated with cell clusters 9 (medial proliferation zone) and 10 (lateral proliferation zone), which house olfactory local and projection interneurons, respectively [5,6]. Pulse-chase double-nucleoside labeling showed definitively that cells labeled with an initial 5-bromo-2′-deoxyuridine (BrdU) pulse left the niche and were found a week later in the proliferation zones, while the second 5-ethynyl-2′-deoxyuridine pulse just before sacrifice consistently labeled first-generation precursors in the stem cell niche [6]. The first-generation neuronal precursors are therefore not self-renewing as proposed for typical stem cells, although these precursors are functionally analogous to neuronal stem cells in the vertebrate brain. In spite of the fact that the first-generation neuronal precursors do not self-renew, the niche is not exhausted and neurons continue to be born throughout the animal's life. The neuronal stem cell niche in crayfish therefore cannot be a closed system, and a major effort in our laboratory recently has been to identify the source of the pre-stem cells that replenish the niche precursor pool.

Studies in our laboratory have shown that cells circulating in the hemolymph, and not cells from other tissues (e.g., hepatopancreas and green gland), are attracted to the neural stem cell niche in vitro [6]. These findings have led to the hypothesis that cells associated with the hematopoietic system and that circulate in the hemolymph may replenish the neuronal precursors in the niche. A close association between the niche and the vasculature is established early, at the time the anlage of the niche appears at the end of embryonic life and in concert with angiogenesis in that region [7]. Morphological and ultrastructural observations confirm that the neurogenic niche in the mature brain is nearly encompassed by blood vessels that are embedded in connective tissues,

[1]Neuroscience Program, Wellesley College, Wellesley, Massachusetts.
[2]Programa de Pós-Graduação em Ciências Morfológicas, Instituto de Ciências Biomédicas, Universidade Federal do Rio de Janeiro, Rio de Janeiro, Brazil.

suggesting a retia-like complex of fine channels between the niche and the vasculature emerging from the underlying accessory lobe [8]. The close association between the niche and vascular system also has been confirmed by experiments showing that dye-labeled dextran injected into the dorsal artery [3] or into the pericardial sinus [6] infiltrates a cavity located centrally in the niche, which has thus been named the vascular cavity. These known relationships between the vasculature and the niche are consistent with the possibility that stem cells circulating in the hemolymph could readily gain access to the niche.

### *The anterior proliferation center*

The recent work of Noonin et al. [9] in the crayfish *Pacifastacus leniusculus* demonstrates that the hematopoietic system in crustaceans is far more extensive than previously recognized. In addition to well-known hematopoietic tissues located dorsally just beneath the carapace and covering the stomatogastric mill, Noonin and collaborators [9] have identified a specialized region of the hematopoietic system that is located near the brain and which they propose constitutes a multipotent stem cell center. This anterior proliferation center (APC) is distinct from the rest of the hematopoietic tissue (HPT) in several ways: The highest rate of BrdU incorporation is in the anterior part of the HPT and the APC. In addition, the majority of cells in the APC contain nuclei with loose chromatin (euchromatin), whereas most cells in the posterior HPT contain cells with condensed chromatin (heterochromatin). It is suggested that this difference in the chromatin structure is related to the degree of differentiation of the cells, with DNA becoming more condensed as the cells differentiate [9,10]. Further, reactive oxygen species (ROS), which induce the differentiation of hematopoietic stem cells in *Drosophila* [11] and in the mammalian myeloid lineage [12], are produced in high levels only in the most anterior part of the HPT, between the APC and the brain [9]. ROS labeling increased throughout the APC at 30 min following laminarin injection into crayfish, a treatment that mimics fungal infection. This timing corresponds with the decrease in circulating hemocytes and subsequent recruitment of new hemocytes from the HPT associated with laminarin treatment, suggesting that increased metabolic activity may be related to the differentiation of cells in the APC. Based on these and additional data, Noonin et al. [9] propose that cells in the APC are the multipotent stem cells of the crustacean HPT. Because of their properties and their location, these cells are of special interest in our efforts to identify the source of first-generation neuronal precursors that produce adult-born neurons.

This article extends the work of Noonin et al. [9] by localizing the APC in the closely related crayfish *P. clarkii*, and by characterizing the cellular organization and behavior of cells in the APC compared with more posterior hematopoietic tissues. Our studies show that the APC is localized within the cor frontale or auxiliary heart (Fig. 1A, B), which provides direct vascular access to the brain and eyes via the cerebral and ophthalmic arteries, respectively. Our data also show that secondary branches from the cerebral artery contact the neurogenic niche and streams, infiltrating these areas. Further, we show that unlike the more posterior HPTs that extend over the gastric mill, regions within the APC are characterized by proliferating cells that form rosette-like structures. In vertebrates, morphologically similar structures called neural rosettes are the developmental signature of neuroprogenitors in cultures of differentiating embryonic stem cells [13,14] and in neurogenic regions in the adult brain, resembling patterns seen in other developing epithelial tissues [15]. Based on these findings, we hypothesize that rosette cells composing the APC are indeed multipotent stem cells and that these are prime candidates to replenish the pool of first-generation neuronal precursors in the neurogenic niche as these divide and their daughters migrate away.

## Materials and Methods

### *Animals*

Adult male and female crayfish *P. clarkii* (carapace length [CL] 15–30 mm) were obtained from Carolina Biological Supply Company and maintained at room temperature in aquaria containing aerated artificial pond water and exposed to a light:dark cycle of 12:12 h. Crayfish of this size are sexually mature adults.

### *BrdU timed series: cell proliferation studies of the APC*

The BrdU (Sigma-Aldrich) labeling reagent (5 mg/mL in saline) was injected (200 μL) into the base of the third walking leg of 12 crayfish (CL 28–30 mm). At four intervals following injection (3, 6, 24, and 72 h), three crayfish were killed and the brain and cor frontale (auxiliary heart) were dissected and fixed overnight in 4% paraformaldehyde in 0.1 M phosphate buffer (PB; pH 7.4) at 4°C. Tissues were rinsed several times in PB with 0.3% Triton X-100 (PBTx) followed by a 30-min treatment in 2 N hydrochloric acid. After rinsing again in PBTx, tissues were incubated for 18 h at 4°C in mouse monoclonal (Clone MoBU-1) anti-BrdU conjugated to Alexa Fluor® 488 (Invitrogen; B35130). After rinsing in PBTx, tissues were treated with the nucleic acid stain propidium iodide (PI; Sigma-Aldrich; 10 μg/mL PB) for 10 min at 18°C–20°C. After rinses in PB, the preparations were mounted in Fluoro-Gel (Electron Microscopy Sciences) and examined and imaged using a Leica TCS SP5 confocal microscope equipped with argon 488-nm and 561-nm and 633-nm diode lasers. Serial optical sections were taken at 0.5–1-μm intervals and saved as both three-dimensional stacks and two-dimensional projections.

### *Detection of ROS and localization of mitochondria*

ROS production in APC tissue and posterior HPT was monitored in live tissues using the protocol of Noonin et al. [9]. Saline (200 μL) was injected into the pericardial sinus of crayfish (~18 mm CL) 1 h before dissection to stimulate a brief hematopoietic response [9]. Posterior HPT and APC tissue were then dissected in oxygenated crayfish saline. Freshly prepared 2′,7′-dichlorofluorescein diacetate (D6883; Sigma) in dimethyl sulfoxide (DMSO; 5 mg/mL; Sigma) was diluted with 0.1 M PB (1:1,000; 10 μM concentration). Whole, dissected HPTs were incubated with the detector for 10 min with gentle shaking in a dark chamber at room temperature. Three 5-min rinses in PB followed by

mounting in 30% glycerol in PB allowed for immediate observation of the tissues with a Nikon 80i fluorescent stereomicroscope.

While there are several nonmitochondrial sources of ROS, mitochondria are major contributors, permanently producing ROS as a by-product of oxidative phosphorylation [16]. MitoTracker® Deep Red (Molecular Probes; FM M22426), a cell-permeant probe, contains a mildly thiol-reactive chloromethyl moiety for labeling mitochondria and is retained in the mitochondria after fixation. We therefore used this agent to localize mitochondria in cells in the APC and posterior HPT, as one indicator of metabolic activity and the potential for higher ROS production. One hour before dissection, saline (200 μL) was injected into the pericardial sinus of crayfish (~18 mm CL) to stimulate a hematopoietic response. A labeling solution of MitoTracker® at a working concentration of 100 μM in crayfish saline was prepared. Freshly dissected tissues ($n=8$) were immersed in the labeling medium for 30 min at 37°C, rinsed in PB, and fixed with 4% paraformaldehyde in PB (pH 7.4), followed by staining with the nucleic acid marker 4′,6-diamidino-2-phenylindole (DAPI; Molecular Probes).

### *Morphological examination of fixed tissue*

The posterior and anterior regions of HPT were carefully dissected from crayfish (CL 20 mm) in cold saline (205 mM sodium chloride, 5.4 mM potassium chloride, 34.4 mM calcium chloride, 1.2 mM magnesium chloride, and 2.4 mM sodium bicarbonate) and fixed overnight in 4% paraformaldehyde (pH 7.4). To maintain the structural integrity of the APC, fix was injected medially into the base of each eyestalk a few minutes before dissection. Tissues were visualized and imaged using an Insight-spot 2 camera coupled to a Nikon SMZ 1500 stereomicroscope.

### *Immunohistochemical localization of tubulins*

Fixed APC tissue and posterior HPT were rinsed multiple times with 0.3% PBTx and incubated overnight at 4°C in either mouse monoclonal anti-β tubulin (1:10; Developmental Studies Hybridoma Bank, No. E7) or mouse monoclonal anti-tyrosinated tubulin (1:1,000; Sigma; T-6557), which reacts with tubulin's carboxy-terminal tyrosine. Tissues were rinsed with 0.3% PBTx for 2 h and incubated in goat anti-mouse IgG Cy2 (1:100; Jackson Immunoresearch) at room temperature for 4 h. After rinsing with 0.3% PBTx, they were counterstained with PI (10 mg/mL; 10 min at 18°C–20°C; Sigma). The samples were then rinsed with PB and mounted with Fluoro-Gel (Electron Microscopy Sciences). Preparations were viewed and images captured with a Leica TCS SP5 confocal microscope.

### *BrdU labeling of cells in the dorsal artery and APC*

Crayfish (CL 15–20 mm) were maintained in pond water containing BrdU (2 mg/mL) for 24 h before sacrifice. Tissues were fixed and processed immunocytochemically as described under the "BrdU timed series: cell proliferation studies of the APC" heading except that the nucleic acid marker DAPI was used instead of PI.

### *Dextran fills of the vasculature*

Labeling of the brain vasculature in crayfish was achieved by injecting fluorescein isothiocyanate (FITC)-conjugated dextran (3,000 MW; Invitrogen; D-3306; 500 μL of a 1 mM solution in crayfish saline) into the pericardial sinus. Animals (15–20 mm CL; $n=5$) were placed in artificial pond water for 5 min following injection. The brain, cor frontale and associated APC were dissected in saline and fixed in 4% paraformaldehyde overnight at 4°C. Using standard immunohistochemical techniques, tissues were labeled with mouse anti-glutamine synthetase (1:100; Becton Dickinson; 610517) followed by overnight incubation in goat anti-mouse CY5 (1:100; Jackson Immunoresearch), and then stained with the nuclear marker PI.

### *Data analyses and statistical treatment*

The numbers of PI- and BrdU-labeled cells were quantified from stacked images obtained with a Leica TCS SP confocal microscope. A single optical section was projected onto the monitor and the labeled cells traced onto a transparent sheet to count the numbers of labeled cells. The area of each APC tissue imaged was standardized so that each region (i.e., a stack) was a 130-$\mu m^2$ region (one optical section at 120× magnification) with a depth of 4 μm. Percentages of BrdU-positive cells and mitotic profiles were calculated relative to the total number of PI-labeled cells and mitotic profiles, respectively. The number of BrdU-labeled rosettes was counted in three different areas bilaterally of the APC (see diagram Fig. 6A). The cor frontale muscles (CFMs), medially located in the APC, were used as a reference point to select these regions. Rosette labeling was classified into three different types: *Center*—only the center cell within the rosette was labeled with BrdU; *Partial*—BrdU labeling in the center cell plus two or three cells around the center cell; and *Full*—all of the cells composing the rosette were labeled. Counts of the rosette types and mitotic profiles were taken at four different time points after BrdU injection (3, 6, 24, and 72 h) and tested for differences using a one-way analysis of variance (ANOVA) followed by Tukey's multiple comparisons (GraphPad Software).

## Results

Because of the potential importance of the hematopoietic system for adult neurogenesis in crustaceans, in the present study we have localized these tissues in the crayfish *P. clarkii*, a species in which mechanisms underlying the production of adult-born neurons have been carefully examined [17]. The posterior HPT in *P. clarkii*, like that described in *P. leniusculus* [9], spreads over and around the stomatogastric mill. The HPT also extends forward toward the brain and part of it can be found lying between the anterior part of the gastric mill and the cor frontale, or auxiliary heart [18,19]; this is the anterior HPT described by Noonin et al. [9] in *P. leniusculus*. Dissections of the cor frontale and confocal examination of fixed tissues in *P. clarkii* also revealed highly proliferative tissue lying *within* the cor frontale. The location, extent of BrdU incorporation, tests for ROS and other morphological features of this tissue in *P. clarkii* lead us to believe that this is equivalent to the APC discovered in *P. leniusculus* [9]. The studies presented here also extend previous findings by characterizing the regional and cellular organization of the APC and examining the

vascular route by which APC cells travel to and access brain tissues.

### *Vasculature associated with the hematopoietic system: nomenclature*

The following account uses the terminology of Steinacker [19] in referring to the blood vessels associated with HPT and the cor frontale. Accordingly, the dorsal median artery (DMA) is the primary median vessel from the heart to the brain, extending anteriorly just beneath the carapace to a point close to the rostrum where it turns ventrally and descends toward the brain (Fig. 1A). Just dorsal to the brain, the DMA distends and forms a relatively large sac (the cor frontale) that encloses the longitudinally-oriented CFMs (Fig. 1B). Three blood vessels emerge from the cor frontale: two lateral vessels (the ophthalmic arteries) go to the optic ganglia in the eyestalks, and a medial branch (the cerebral artery, CA) projects to the brain. Historically, a variety of terms have been used by various authors in referring to these vessels, with no general consensus as to their assignments. Thus, the DMA also has been called the median artery [18,20,21] or the ophthalmic arteries [22–24], the latter of which is easily confused with the true ophthalmic arteries servicing the eyes and which emerge from the cor frontale. Because HPTs are intimately associated with these vessels, the designations of Steinacker [19] will be used in this article, as these terms are unambiguous and permit a precise assignment of location.

### *Organization of HPTs in P. clarkii*

Most crustacean species have a distinct hematopoietic organ that is composed of a series of ovoid lobules that collectively form a thin sheath of connective tissue, found in close proximity to the DMA as it extends on the dorsal surface of the foregut just beneath the carapace (hereafter referred to as the posterior HPT; Fig. 1A, B). In *P. clarkii*, HPT is located in this typical position, as in *P. leniusculus* [24] and other species [22]. Proliferating hematopoietic cells (HPCs) tend to be located at the edges of the HPT (Fig. 1D), from which they are released into the surrounding sinus. In *P. clarkii*, cells composing these lobules range in size from 10 to 15 μm.

Two other distinct regions of HPT, the anterior HPT and the APC (Fig. 1A, B), recently described in *P. leniusculus* [9], are readily identifiable in *P. clarkii* on the basis of location and relative levels of proliferative activity. At roughly the position where the dorsal artery distends to form the cor frontale, the HPT forms extensions, defined by Noonin et al. [9] as the anterior HPT (Fig. 1A, B). Cells in the anterior HPT in *P. clarkii* are organized similarly and are of the same size as cells in the posterior HPT.

The APC, which Noonin et al. [9] report as being connected to the brain, is readily identifiable in *P. clarkii*. Timed studies were conducted where the S-phase marker BrdU was injected into crayfish, followed by sacrifice of groups of crayfish at 3, 6, 24, and 72 h post-injection (Fig. 2). These time points were chosen to occur after any transient evoked hematopoietic response, which peaks by ~1 h after injection of fluid [25,26]. It should be noted that the BrdU clearing time in *P. clarkii* is relatively long, between 30 and 48 h [6], and therefore the increasing times between 3 and 24 h represent longer exposures to BrdU, while the 72-h time point would

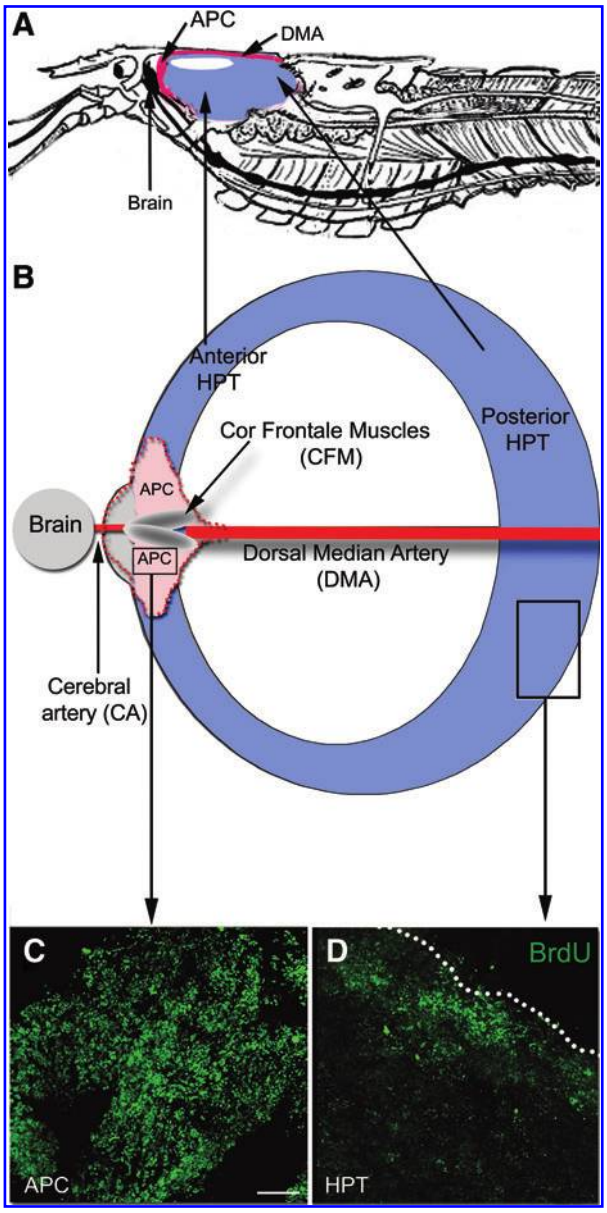


**FIG. 1.** Location and proliferative characteristics of *P. clarkii* hematopoietic system. **(A)** Anterior and posterior hematopoietic tissues (HPT, *blue*) in the crayfish relative to the dorsal median artery (DMA, *red*). The anterior proliferation center (APC, *pink*) is located just anterior and ventral to the HPT, within the cor frontale (auxiliary heart), which supplies the brain and eyes with hemolymph via the cerebral and ophthalmic arteries, respectively. **(B)** The posterior and anterior HPT, APC, and the brain are shown diagrammatically in a flattened view where anterior structures are at the *left* and posterior to the *right*. The DMA (*red*) extends from the heart (not shown) dorsally just beneath the carapace on the surface of the foregut. Posterior HPT (*blue*) is located laterally on either side of the DMA, which expands to form the cor frontale anteriorly (*red dotted line*), just dorsal to the brain. APC tissues (*pink*) are located inside the cor. The cerebral artery (CA, *red*) emerges from the cor and provides the only blood supply to the brain. **(C, D)** Images of 5-bromo-2′-deoxyuridine (BrdU) labeling (after a 6-h BrdU incubation) at low magnification illustrate the high degree of cell cycle activity throughout APC tissues **(C)**, while dividing cells are localized to the edges of the posterior HPT **(***dotted line*, **D)**. Scale bar is 100 μm for **(C)** and refers also to **(D)**. Color images available online at www.liebertpub.com/scd

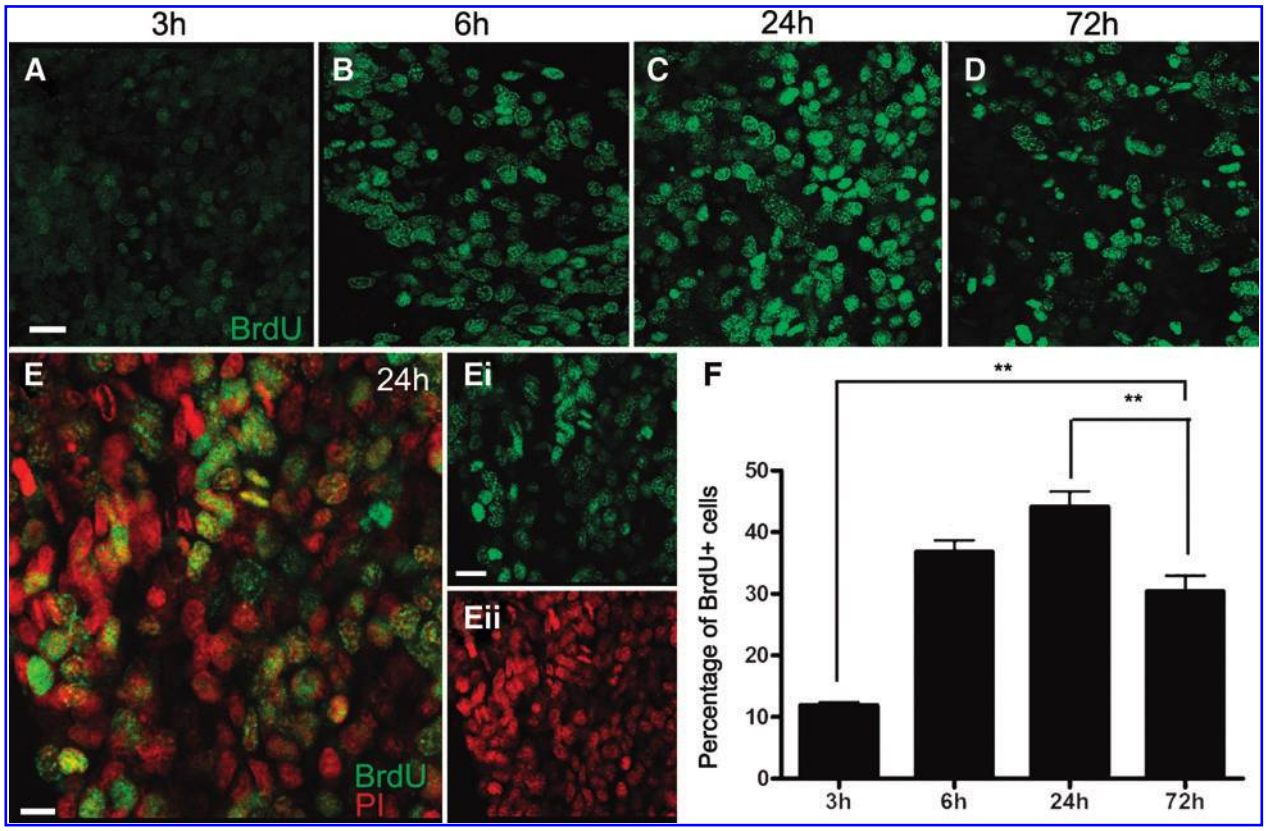


**FIG. 2.** BrdU labeling of cells at four time points following injection of BrdU into adult crayfish. **(A)** 3, **(B)** 6, **(C)** 24, and **(D)** 72 h. Images illustrate the increasing proportion of labeled cells until 24 h, and the decrease in the number of BrdU-labeled profiles at 72 h. An example of BrdU (*green*) and propidium iodide (PI, *red*) double labeling is shown in **(E)**, with individual channels shown in **(Ei)** (BrdU) and **(Eii)** (PI). **(F)** A graph of the percentage of BrdU-labeled cells relative to total cell counts derived from PI labeling. Scale bars are 15 μm for **(A–D)**, 10 μm for **(E)**, and 20 μm for **(Ei)** and **(Eii)**. Color images available online at www.liebertpub.com/scd

have occurred after the available BrdU had cleared. More than 10% of cells in the *P. clarkii* APC label 3 h after BrdU injection (Fig. 2A, F), and 40%–45% of cells label with BrdU at 24 h post-injection (Fig. 2C, F). The highest percentages of mitotic figures were labeled at the 6- and 24-h time points (Fig. 3), which suggests that the time from S- to M-phase is at least 6 h long. Alternatively, the maximal BrdU labeling of mitotic figures at the 24-h time point could reflect multiple divisions of cells with a shorter cell cycle, and therefore may represent accumulated, multiple generations. The vast majority of cells in the APC range in size from 8 to 12 μm, with occasional cells reaching up to 20 μm; these unusually large

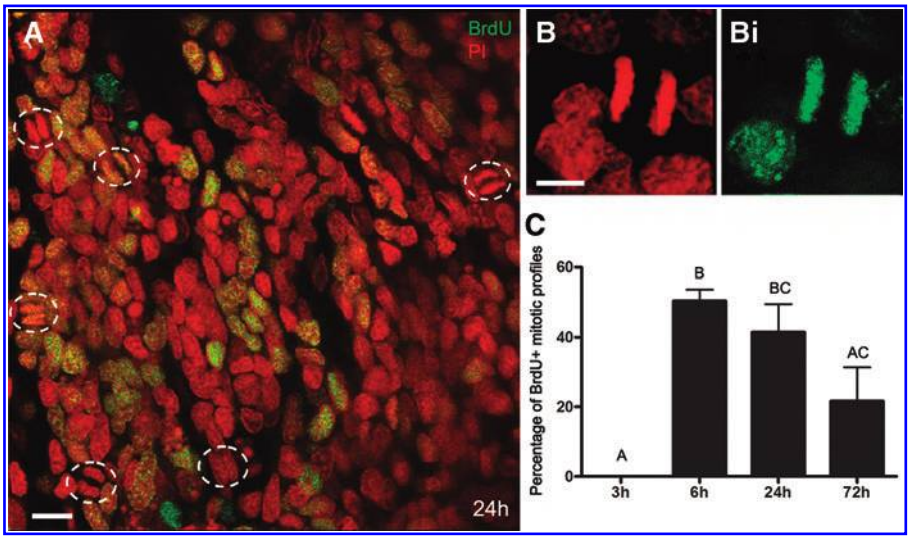


**FIG. 3.** The percentage of mitotic profiles increases to a maximum at 24 h. **(A)** An image of APC tissue at the 24-h time point, showing six clearly labeled mitotic profiles (*dotted circles*); PI (*red*); BrdU (*green*). **(B)** is a higher magnification of one mitotic figure labeled with PI **(B,** separated channel from image in **A)** and BrdU **(Bi,** separated channel from image in **A)**. **(C)** Graph of quantitative data for the percentage of BrdU + mitotic profiles relative to total PI mitotic profile counts. Scale bars are 10 μm for **(A)** and 5 μm for **(B)**. Color images available online at www.liebertpub.com/scd

cells are often labeled with BrdU, and probably represent cells that have duplicated their DNA and grown in size in preparation for mitosis.

### *ROS labeling in the APC and posterior HPT*

The production of ROS, which is indicative of the metabolic state of cells, was monitored in live APC tissue and posterior HPT treated with 2′,7′-dichlorofluorescein diacetate. High levels of ROS production were detected in the APC, but ROS activity was not detected in the brain (Fig. 4A). A weak ROS signal was limited to the peripheral margins of the posterior HPT.

MitoTracker® was used to label mitochondria in live tissues followed by fixation, as another indicator of metabolic activity and the potential for higher ROS production. APC cells contained intense MitoTracker® labeling (Fig. 4B, C), a finding that parallels the detection of high ROS levels in this tissue (Fig. 4A) [9]. Cells were particularly intensely labeled in the region on top of and between the CFMs (Fig. 4C).

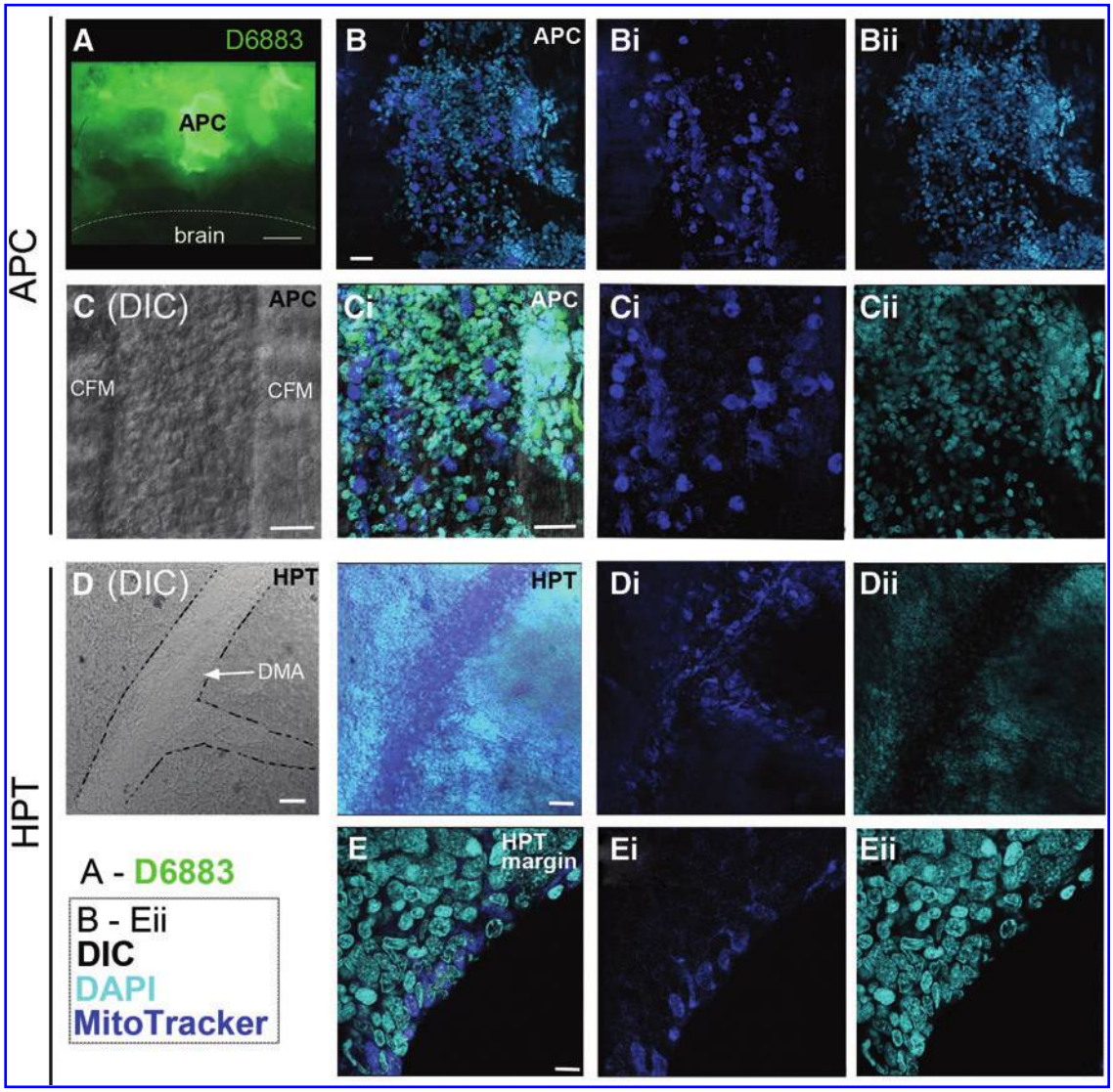


**FIG. 4.** Labeling of reactive oxygen species (ROS) and mitochondria in APC and HPT cells. **(A)** Detection of real-time ROS production (*green*) in live APC and brain tissues using D6883 (2′,7′-dichlorofluorescein diacetate) shows extensive ROS production in the APC after injection of saline into the dorsal sinus. Labeling of mitochondria in APC tissue **(B, C)** and posterior HPT **(D, E)** detected with MitoTracker® Deep Red FM (*blue* [pseudocolor]) and stained with 4′,6-diamidino-2-phenylindole (DAPI, *cyan*), following saline injection into the dorsal sinus. **(C, D—DIC)** Differential interference contrast (DIC) confocal microscopy identifies areas of interest within the APC and HPT. **(B)** Stacked confocal images of the APC in an area next to the cor frontale muscles (CFMs) with separate channels shown in **(Bi)** and **(Bii)** (*cyan*, DAPI; *blue*, MitoTracker®) reveal many cells containing intense MitoTracker® labeling. Increased magnification **(C–Cii)** illustrates individual cells between the two cor muscles. In contrast, there are many fewer cells that label for MitoTracker® (*blue*) in the HPT **(D, E)**. Most of the labeling occurs in the DMA (*arrow* in **D [DIC]**) or in branches from the DMA **(D–Dii)**. Moderate MitoTracker® labeling is observed in cells along the lateral margins of the HPT **(E–Eii)**. Scale bars are 500 μm for **(A)**, 100 μm for **(B–Bii)**, 50 μm for **(D–Dii)**, and 10 μm for **(E–Eii)**. Color images available online at www.liebertpub.com/scd

In parallel with high levels of BrdU labeling along the lateral margins of the posterior HPT (Fig. 1D), a few cells in this same location contained moderate levels of MitoTracker® labeling (Fig. 4E). More central regions of the posterior HPT were not labeled, suggesting that metabolism and cell cycle activity are maximal at the margins of this tissue, as previously reported by Noonin et al. [9]. MitoTracker® also labels cells in the DMA (Fig. 4D, Di) and in small vessels connected to the DMA, suggesting that cells circulating in the hemolymph maintain high metabolic activity, perhaps because they are undergoing their final differentiation [24] or a few cells may still be in the cell cycle.

The high degree of cell cycle activity in cells near and surrounding the CFMs, their location between the anterior HPT and the brain, and high levels of ROS and mitochondrial labeling in *P. clarkii* are consistent with characteristics of the APC in *P. leniusculus*, thus confirming the identity of this tissue as equivalent to the APC described by Noonin et al. [9].

### *The APC in P. clarkii is located within the cor frontale*

A striking feature of the APC in *P. clarkii* is its location inside the cor frontale (Fig. 5). In preparations where the brain, cor frontale, and all three regions of the *P. clarkii* hematopoietic system (posterior HPT, anterior HPT, and APC) were dissected and laid flat for observation (Fig. 5B–D), the spatial relationships between these tissues could be examined. APC tissue wraps around and between the CFMs (Fig. 5B, D) and sheets of cells (Fig. 5A, purple; B, C, dotted outline) form lateral extensions attached to the dorsal and ventral walls of the cor frontale. The CFMs originate within the rostrum on the dorsal carapace and are anchored caudally to a fibrous strap lying across the dorsoanterior edge of the brain. Two fine ligaments extend posteriolaterally from the caudal ends of the muscles. The cor frontale itself extends sideways, ventral to the large muscle blocks holding the gastric mill anteriorly in the animal, and attaches laterally to the exoskeleton (see Fig. 5E). In studies where saline was injected into the cerebral artery to inflate the cor frontale, it was very clear that the sheer membrane to which APC cells are attached forms the walls of the cor frontale.

The localization of the APC inside the cor frontale is of major interest because there are only three exits from this auxiliary heart: two lateral exits, the ophthalmic arteries, which supply blood to the optic neuropils contained in the eyestalks (Fig. 5E); caudally, a single median vessel, the cerebral artery, supplies blood to the brain (Fig. 5E, F) [19]. Therefore, all of the blood that reaches the cor frontale, which is most of that pumped from the heart into the DMA, will pass through the neural tissues in the optic and brain neuropils; moreover, it is important to recognize that the cerebral artery provides the entire blood supply to the brain. Significantly, the only regions identified in the crustacean nervous system where neurogenesis continues throughout adult life, are in cell clusters 9 and 10 in the brain [3,17] and in the eyestalks [27]. These relationships will be addressed further in the Discussion section.

### *Cellular organization of the APC*

The APC is different from the rest of the HPT not only due to its distinctive location, but also in its cellular composition and organization. Cells composing the anterior and posterior regions of the HPT are arranged in lobules that contribute to large sheets of tissue, with no obvious cellular pattern. In contrast, APC cells located near the CFMs (regions A and B, Fig. 6A) are organized into rosette-like configurations; very few rosettes are found in region C, where most cells are organized in sheets without any obvious pattern. However, cells in all three regions are equally labeled with BrdU. Our observations suggest that the majority of cells in regions A and B participate in rosettes, although these are in different orientations in the tissue and therefore all cannot be visualized in confocal stacks viewed in a single plane. All members of the rosettes can be of similar size (8–12 μm), although sometimes, the central cell within the rosette is noticeably larger than those forming the outer circle. BrdU labeling suggests that the cells composing the rosettes may have a lineage relationship, because short-term (6 h) exposure to BrdU generally labels only the central cell in the rosette (Fig. 7A, B) while a 72-h exposure tends to label all members of the rosettes (Fig. 7E, F), even though BrdU would have cleared from the system by 30–48 h. This temporal pattern of labeling suggests that the surrounding cells could be progeny, labeled during the S-phase of the central mother cell. However, it also is clear that the outer cells can undergo unrelated division, as they are occasionally labeled with BrdU, while the central cell is not.

Immunocytochemical studies of the posterior HPT and the APC were conducted with antibodies against β-tubulin and tyrosinated tubulin, providing some points of morphological comparison between these tissues. Microtubules are primarily formed from α- and β-tubulin, the most common members of the tubulin family. Tubulins also are subjected to post-translational modifications, one of which involves the cyclic removal of the carboxy-terminal tyrosine of α-tubulin by a carboxypeptidase and the re-addition of a tyrosine residue by the tubulin–tyrosine ligase [28].

The most notable aspects of β-tubulin labeling are the observations that β-tubulin labels a scaffold or cage encircling rosette complexes, and that rosettes are frequently tethered to each other via β-tubulin immunoreactive fibrils (Fig. 8A, B). Dividing cells in the rosettes often have fibrous extracellular extensions connecting mitotic profiles in neighboring rosettes to one another (Fig. 8A, Ai). β-Tubulin immunoreactivity in the posterior HPT also reveals fibrous elements that form a web within which the HPCs are nestled (Fig. 8C, D). Cells in the process of dividing are intensely immunoreactive for β-tubulin (Fig. 8C).

Antibodies generated against tyrosinated tubulin label very different elements in the APC and posterior HPT than those immunoreactive for β-tubulin. In the APC, tyrosinated tubulin immunoreactivity is found in the cytoplasm of cells composing the rosettes (Fig. 8F). Other cells that are not obviously contributing to a rosette also are encircled by tyrosinated tubulin labeling (Fig. 8E). In contrast, tyrosinated tubulin immunoreactivity is found in fibrous elements in the posterior HPT (Fig. 8G, H), as well as in the cytoplasm of what appear to be bipolar cells (Fig. 8H, arrow). Fibers closely resembling these label the early protoniche during development, at the time of hatching [7].

### *Access to the neurogenic niche*

The DMA posterior to the cor frontale and the cerebral artery emerging from the cor frontale were examined in

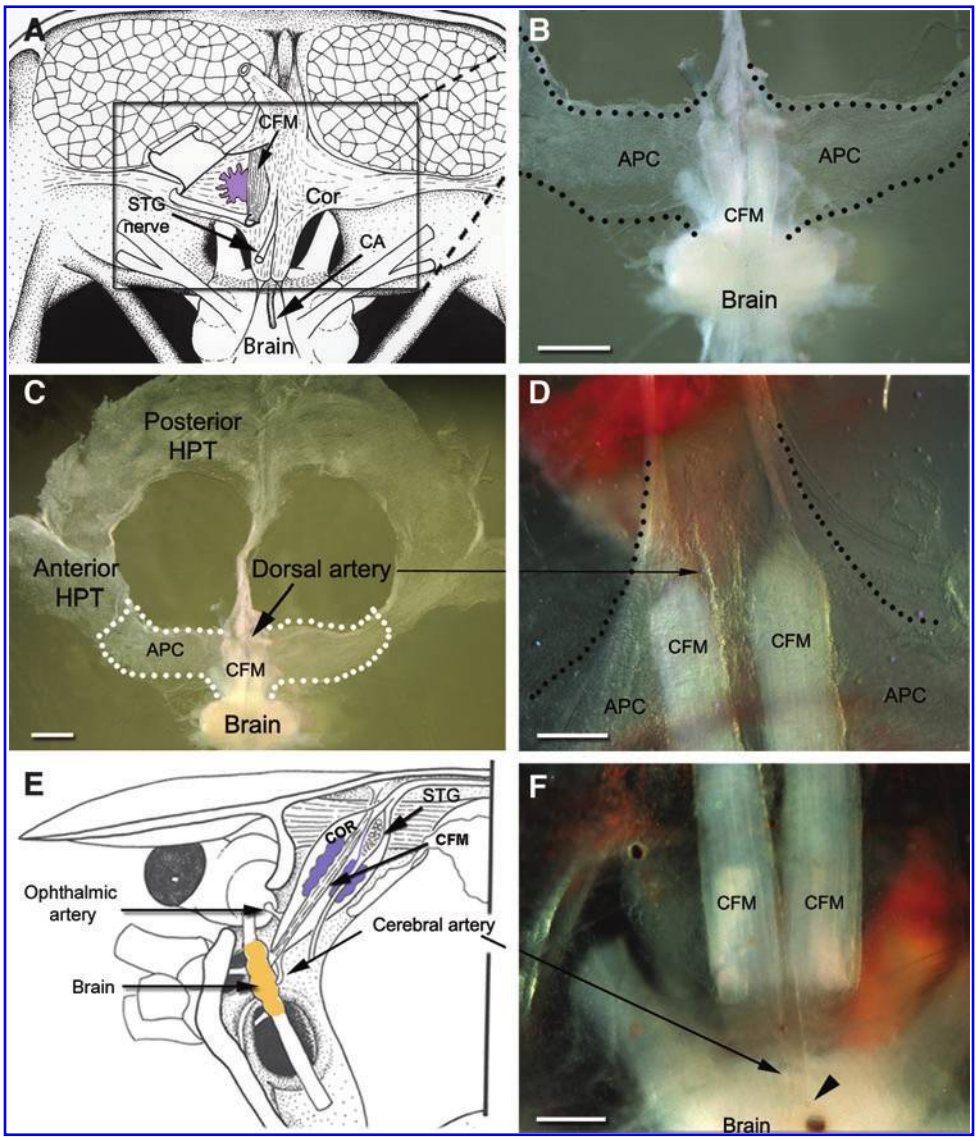


**FIG. 5.** Localization of APC tissues. **(A)** Scale drawing of the APC within the cor frontale. *Right side*: cor is shown in a dorsal view. *Left side*: the dorsal membrane of the cor is peeled away to reveal the APC (*purple*) inside the auxiliary heart. **(B–D, F)** A stereomicroscope was used to photograph the brain and APC (area indicated in *box* in **A**), after dissection of the cor and brain from the head of the crayfish. The APC tissue within the cor has been spread out and flattened to reveal the relationship of this tissue with the CFMs **(B, D)**. The dorsal artery can be visualized entering the cor **(C, D;** *arrow***)**, and the cerebral artery exiting the cor **(F,** *arrow***)**. APC tissue (outlined with a *dotted line* in **B–D**) is located around and between the CFMs, as well as attached to the walls of the cor frontale **(B–D)**. **(E)** A scale drawing of a side view of the crayfish head, illustrating the position of the APC (*purple*) within the cor, and the positions of the brain (*yellow*), cerebral and ophthalmic arteries that run from the cor frontale, and stomatogastric ganglion (STG). **(F)** The emergence of the cerebral artery and its insertion point (*arrowhead*) on the dorsal surface of the brain can be visualized. Scale bars are 500 μm for **(B)** and **(C)**; and 200 μm for **(D)** and **(F)**. **(A)** and **(E)** are original drawings by D.C. Sandeman. Color images available online at www.liebertpub.com/scd

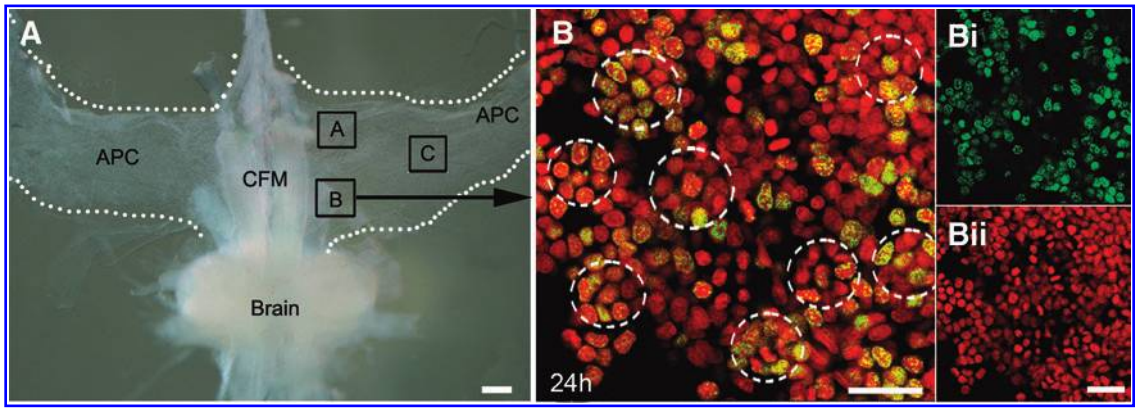


**FIG. 6.** APC cells are arranged in rosettes near the midline and CFMs. **(A)** APC tissue was observed in three regions: A, B, and C (indicated in *boxes*). **(B)** Cells were arranged in rosettes (*dotted circles*) in areas A and B, near the CFMs, labeled with BrdU **(Bi)** and PI **(Bii)**. Scale bars are 200 μm for **(A)**; and 30 μm for **(B, Bi, Bii)**. Color images available online at www.liebertpub.com/scd

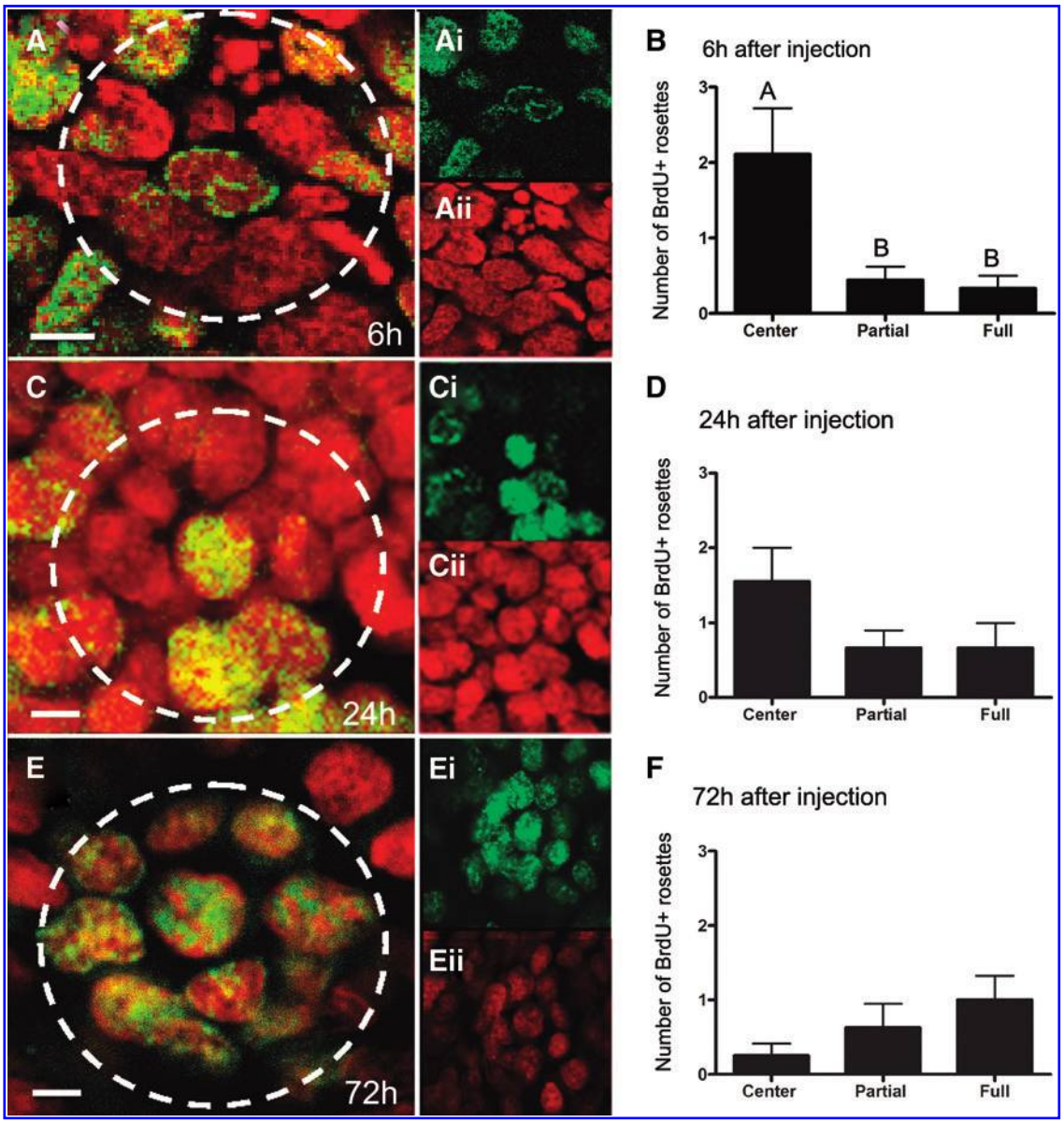


**FIG. 7.** Temporal studies of BrdU labeling within rosettes (*dashed lines*) suggest that cells have a lineage relationship. **(A, B)** Six hours after BrdU injection, central cells within rosettes are disproportionately labeled, while surrounding cells are generally not labeled. **(C, D)** By 24 h after BrdU injection, the relative proportions of partial and full rosettes compared with central cell labeling tend to increase. **(E, F)** By 72 h after BrdU injection, rosettes are generally fully labeled—both center and surrounding cells. Scale bar is 5 μm for **(A, C,** and **E)**. **(Ai, Aii, Ci, Cii, Ei,** and **Eii)** are the separated channels for confocal images **(A)**, **(C)**, and **(E)**, respectively. Color images available online at www.liebertpub.com/scd

BrdU- and DAPI-labeled preparations to observe the prevalence of S-phase cells found within these structures (Fig. 9). A few elongated, BrdU-labeled cells 8–15 μm in their largest dimension were found in the DMA in the region just posterior to where the artery expands to form the cor frontale (Fig. 9, regions 2 and 3). Because of their position and size, these are likely to be hemocytes that were labeled during their final division in the HPT, and which were then released into the circulation. Hemocytes do not divide after they are released from the HPT [29]. Many more BrdU-labeled cells of various sizes also are observed in the area between the CFMs, in the region where the cerebral artery that connects the cor frontale with the brain emerges (Fig. 9; regions 4a–d). This provides evidence that cells emerging from the APC may contribute to the cellular population that flows from the cor frontale into the brain.

The cerebral artery emerges from the cor frontale and enters the brain through the dorsal surface (Fig. 5F), where it extends ventrally into two large lateral branches that ramify in the olfactory lobes, accessory lobes, antenna II neuropils, and other smaller neuropil areas (Fig. 10A–C). Afferent vessels project directly from the lateral branches and can be traced to the bilateral neurogenic niches and streams lying on the ventral surface of the accessory lobes (Fig. 10C, D). It is clear from confocal sections through the neurogenic niche that fine capillaries infiltrate the niche and several converge on the vascular cavity, where these appear to terminate (Fig. 10D). Semithin sections through the neurogenic niche also

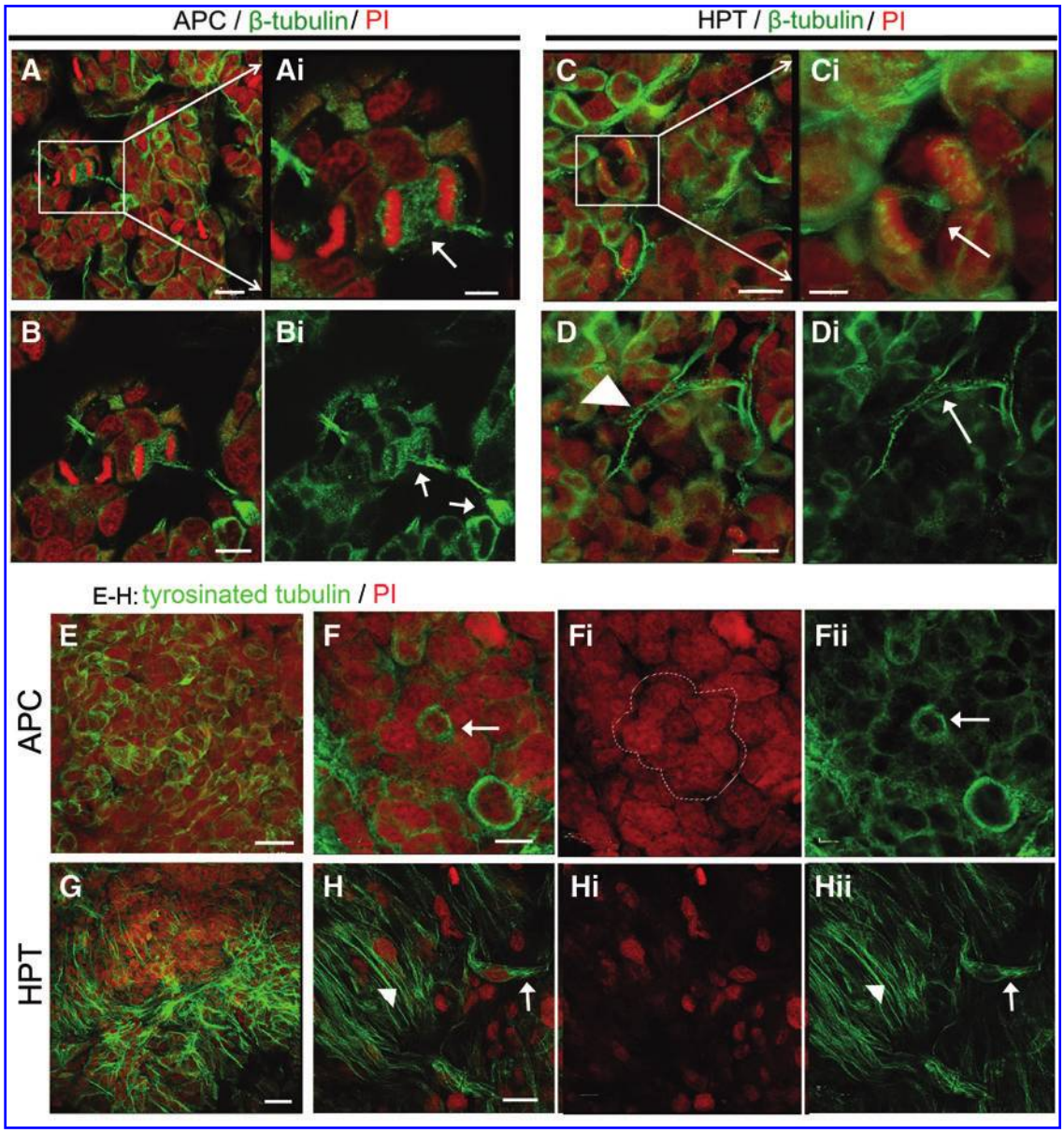


**FIG. 8.** Comparison of the distributions of β-tubulin and tyrosinated-tubulin immunoreactivities in APC tissue and HPT. **(A)** β-Tubulin (*green*) and PI (*red*) labeling reveals three-dimensional cage structures encircling rosette complexes. **(Ai)** High magnification of **(A)** (region in the *white box*), showing β-tubulin distribution in microtubular elements (*arrow*) during mitosis. **(B)** Dividing cells in the rosettes appear to have extracellular extensions (*arrows*) that connect to other mitotic profiles outside of their rosette; rosettes appear to be tethered to each other. **(Bi)** β-Tubulin channel, with *arrows* pointing to a fibrous extension connecting two dividing cells. **(C, D)** In the HPT, aggregates of cells **(***arrowhead*, **D)** and mitotic cells **(Ci,** *arrow***)** are labeled for β-tubulin (*green*) and PI (*red*). β-Tubulin-labeled fibers connect between groups of cells. *Arrow* **(Di)** points to long fibrous extensions. **(E–H)** Tyrosinated tubulin (t-tubulin) antibodies label different microtubular elements in the APC **(E, F)** and HPT **(G, H)**. In the APC, t-tubulin (*green*) is expressed in the cytoplasm, most intensely in the center cell of the rosettes **(F,** *arrow***)**, although other cells are also labeled **(F, Fii)**. With increased labeling in the center cell, rosettes are readily identifiable; PI-labeled rosette is outlined in **(Fi)** (*dotted line*). In the posterior HPT **(G, H)**, fibrous extensions (t-tubulin, *green*) are distributed throughout the tissue. In some examples, individual cells **(H, Hii,** *arrow***)** are distinct from the fibrous background. These fibers may be extracellular extensions of cytoplasmic microtubules **(H, Hii,** *arrowhead*). **(Hi)** Separate channel shows PI-labeled HPT cell (*red*); rosette structures were not found. Scale bars are 15 μm for **(A, B, Bi, C, D, Di)**, 5 μm for **(Ai, Ci)**, 20 μm for **(E, H, Hi, Hii)**, 10 μm for **(F)**, and 40 μm for **(G)**. Color images available online at www.liebertpub.com/scd

show a distinctive cell type with a prominent nucleolus and dispersed chromatin concentrated around the edge of the nucleus in high numbers in connective tissue lying between the niche and accessory lobe (Fig. 10E). Cells with these same characteristics are observed in blood vessels that penetrate APC tissues (Fig. 10F).

## Discussion

The HPTs in the crayfish *P. clarkii* are organized similarly to other decapod crustaceans [22–24], with the major hematopoietic organ located in lobules attached to a thin layer of connective tissue on the dorsal and dorsolateral surfaces of

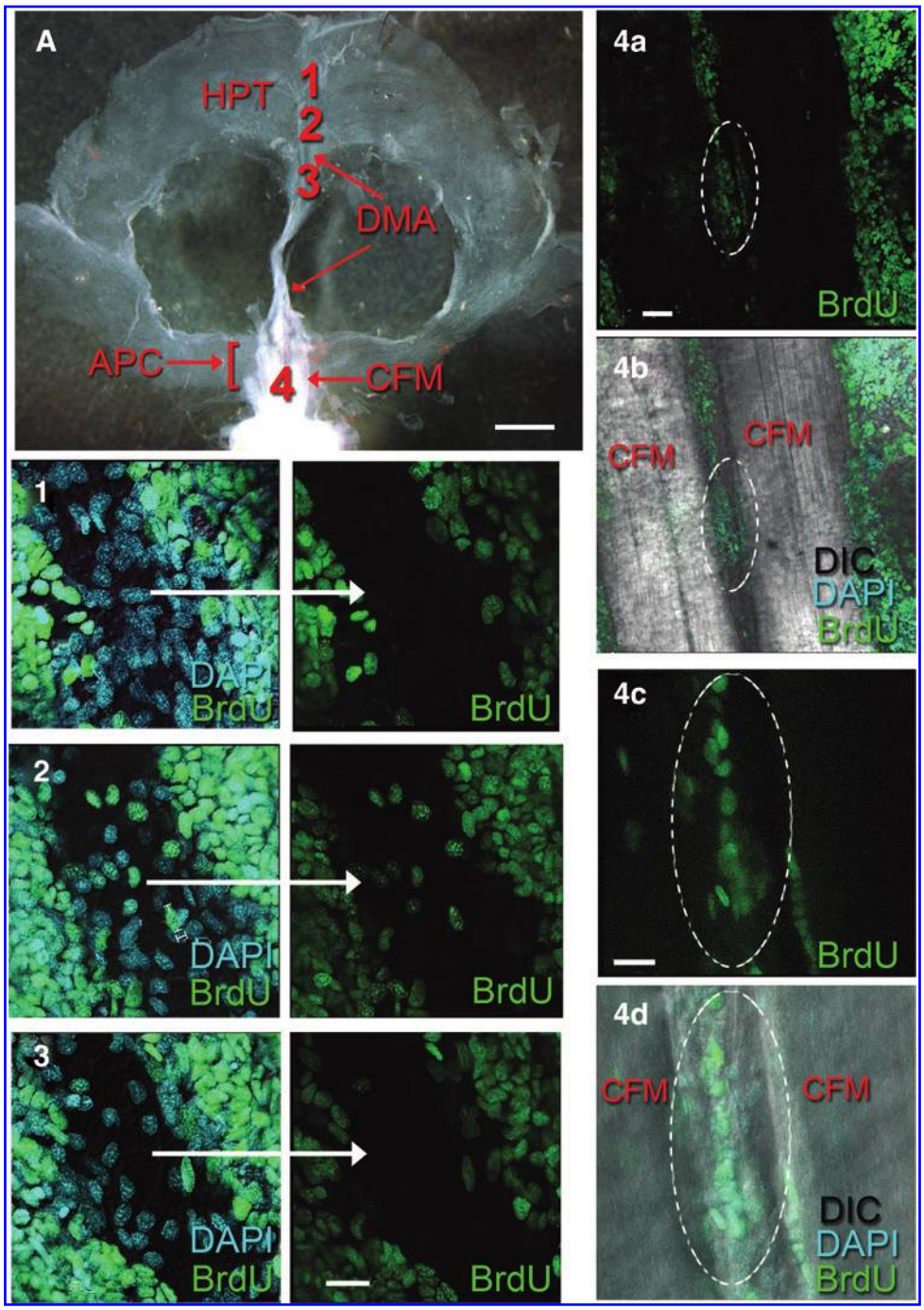


**FIG. 9.** Regions along the DMA were examined following a 24-h BrdU incubation. **(A)** The DMA in the HPT **(A, 1–3)** and regions between the CFMs **(4a–d)** in the APC were examined to identify BrdU-labeled cells in the vasculature. **(***Panels* **1–3)** Many cells (DAPI, *cyan*) are found in the DMA, but few of these are labeled for BrdU (compare *left* and *right panels*). In a section in the ventral APC **(**see **A, 4a–d)** between the cor frontale muscles (CFM; *oval dotted line*) near where the cerebral artery emerges, many more nuclei (DAPI) are double labeled with anti-BrdU antibody (**4c, d** are magnifications of the region in **4a, b**). Scale bars are 500 μm for **(A)**, 10 μm for (**1–3**, shown in 3, *right panel*), 50 μm for **(4a–4b)**, and 20 μm for **(4c–4d)**. Color images available online at www.liebertpub.com/scd

the stomach and surrounding the DMA. The recent work of Noonin et al. [9] in *P. leniusculus* shows, however, that this long-recognized hematopoietic organ is only one part of a much more extensive hematopoietic system. Their work confirms that the lobular tissues composing the posterior HPT are responsible for hemocyte production, as previously demonstrated in several crustacean species [23,24,30]. However, the APC, which they discovered lying near the brain, appears to be a region where multipotent stem cells of the HPT are concentrated. They propose this based on several lines of evidence, including the high level of proliferation in the APC compared with the posterior HPT and loose euchromatin in cells of the APC relative to the more highly condensed chromatin in cells of the anterior and posterior HPT. Unlike cells of the posterior HPT that form monolayers in culture, divide sporadically and differentiate into granular and semigranular precursor cells in vitro after induction [26,31], cells of the APC when cultured divide and form densely packed cell clusters after 3–7 days, some forming bowl-shaped formations. However, after about 2 weeks in culture, these APC-derived clusters stopped growing and did not differentiate, even when cytokines (astakine1 and 2) that influence posterior HPT cell differentiation were added. Noonin et al. [9] have proposed that the location of the APC near the brain may facilitate physiological communication between this tissue and the brain, for example, perhaps by

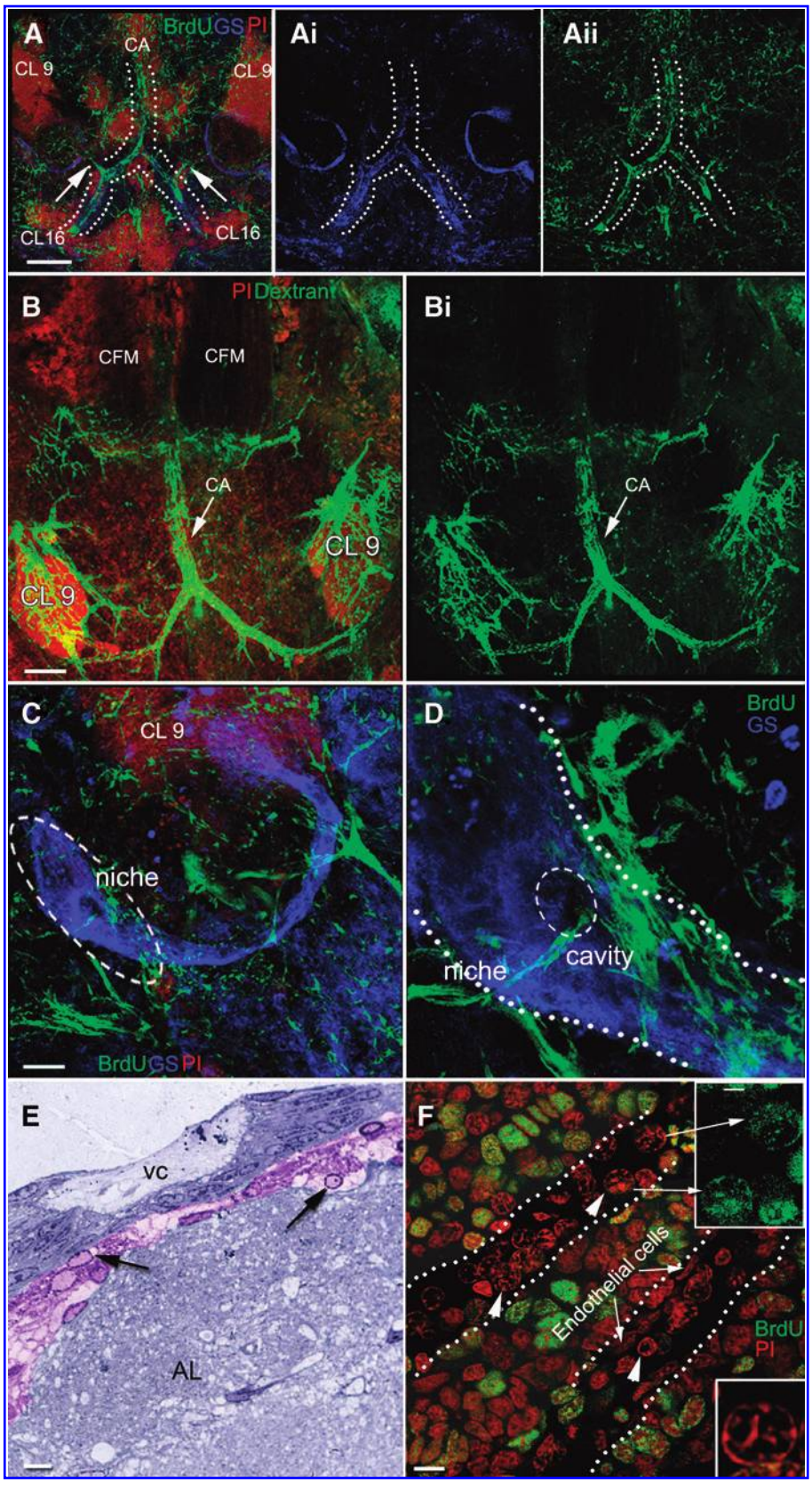


**FIG. 10.** Dextran labeling of the brain vasculature. The brains used in this experiment were not desheathed to examine vascular connections that might be disrupted by removal of the outer membranes enclosing the brain. **(A)** A dorsal view of the brain shows the dextran-filled cerebral artery (CA; *green*; see **Aii**) inserting into the brain. Anti-glutamine synthetase (anti-GS) (*blue*) and PI (*red*) are also shown. Within the brain are two large, dextran-filled bilateral vessels (*dotted line*) projecting toward cell cluster 16 (CL 16), from which afferent vessels branch and extend toward the niche and migratory streams (*arrows*; see also **C** and **D**). Blood vessels within the brain label for GS (*blue*; **Ai**), as do the niche and streams. **(B)** Higher magnification of the brain shows the CA below the CFMs, with its insertion just below the *arrow*. Vessels extend bilaterally toward cluster 9 (CL9), which is highly vascularized as seen by dextran (*green*) in **(Bi)**. **(C)** The neurogenic niche (*dashed-line circle*) labeled for GS (*blue*) has several capillaries strongly labeled with dextran (*green*). Confocal sections through the brain revealed fine capillaries infiltrating in the niche, some of these converging on the vascular cavity, better seen in high magnification **(D)** *green* labeling inside the *dashed-line circle*; *dotted line* marks the boundaries of the niche. In a previous article [8], semithin sections of the niche showed cells resembling hemocytes (*arrows*) in the connective tissue (ct) lining the dorsal side of the niche **(E)**. These had a distinctive nuclear morphology characterized by scarce heterochromatin organized in a ring around the edge of the nucleus, a prominent nucleolus and clear cytoplasm. Similar cells (*arrowheads*) were found in the APC **(F)**, within the blood vessels (*dotted lines*) infiltrating the APC; some also were labeled for BrdU (*green*, *inset*). Endothelial cells (*arrows*) can be observed lining the wall of the blood vessel. AL, accessory lobe; vc, vascular cavity. Scale bars are 200 μm for **(A)**, 150 μm for **(B)**, 50 μm for **(C)**, 20 μm for **(D)**, 10 μm for **(E)**, and 10 μm for **(F)**. **(E)** adapted from [8]. Color images available online at www.liebertpub.com/scd

providing a source of neuronal precursor cells that will generate adult-born neurons. Because our primary interest is in adult neurogenesis in the crustacean brain, we therefore pursued this idea and have localized and examined the components of the hematopoietic system in the model we utilize, the crayfish *P. clarkii*.

The studies presented here demonstrate that all three regions of HPT described by Noonin et al. [9] are readily identifiable in *P. clarkii*: the posterior HPT, anterior HPT, and the APC. As in *P. leniusculus*, APC cells in *P. clarkii* have far more proliferative activity relative to the posterior HPT. High ROS production and intense mitochondrial labeling are found in cells throughout the APC. MitoTracker® labeling was localized at the lateral borders of the posterior HPT, as was BrdU, and in cells within the DMA. We also have discovered that the APC in *P. clarkii* is located within the cor frontale, which vascularizes the brain via the cerebral artery and the eyes via the ophthalmic arteries. Further, we show that APC cells can gain access to the neurogenic niche via capillary branches from the cerebral artery. These vessels have not been noted in earlier studies because we generally remove the sheath covering the brain after fixation and before immunocytochemistry, to facilitate antibody penetration. However, when the ventral sheath is left intact, a series of superficial vessels that infiltrate the niche are revealed (e.g., Fig. 10C, D).

The presence of such proliferative tissues within the cor frontale is of considerable interest because precursor cells released from this tissue would pass immediately to the brain and eyestalk neuropils, both of which contain regions that have the capacity for life-long neurogenesis [17,27]. As suggested by Noonin et al. [9], the APC may indeed be a source for multipotent stem cells which, in the case of adult neurogenesis in the brain of *P. clarkii*, must come from a source extrinsic to the neurogenic niche.

The cor frontale in *P. clarkii* is similar in location and morphology to that found in related crustacean species (e.g., the spiny lobster [*Panulirus interruptus*] and crabs [*Callinectes sapidus*, *Scylla serrata*, *Cancer productus*, and *Cancer antennarius*]) [19]. The cor frontale also contains the stomatogastric ganglion, which is located between the two CFMs. These features of the auxiliary heart are highly uniform among decapod crustacean species, and thus, we suspect that the presence of the APC within this structure is also likely to be a consistent finding.

The cells of the APC are distinctive from cells in the rest of the HPT in that APC cells are distributed in multilayered sheets rather than in lobules, and these are attached to the muscles deep within the cor frontale as well as to the dorsal and ventral membranes that form the cor frontale. In addition, many APC cells are organized in rosette-like structures; these formations were not observed in either the anterior or posterior HPT. The generation of these structures in vivo may correspond to the behavior of APC cells in culture described above, where bowl-shaped cell clusters form.

The APC rosettes are of particular interest because these types of cellular structures have been associated with early stages of neural development and the formation of epithelial tissues in both vertebrates and invertebrates. During neural differentiation, human and mouse embryonic stem cells go through morphogenic events that result in the formation of radially organized columnar epithelial cells called neural rosettes. Cells in these structures label with a variety of neuroectodermal markers and are believed to represent early-stage neural stem cells that have the capacity to form many cell types in the developing brain. Rosettes also form in vitro from embryonic stem cells. The formation of rosettes during gastrulation in *Drosophila* has been related to the establishment of polarity in epithelial cells [32], while rosette structures in zebrafish give rise to neuromasts of the lateral line [33]. In these examples, rosettes are typically organized around zones of cell–cell contact where apical ends undergo a coordinated constriction, such as in the early formation of the neural tube. Mammalian embryonic neural stem cells in culture form rosettes [13], and a similar pinwheel structure is associated with the subventricular zone in mice that is responsible for adult neurogenesis of olfactory interneurons [15]. Elkabetz et al. [14] suggest that neural rosettes derived from human embryonic stem cells (R-NSCs) may represent the first neural cell type capable of recreating the full cellular diversity of the mammalian nervous system, thus implying that these assemblies of cells represent stem cells with a broader potential than traditional neural stem cells, whose lineage is generally restricted to specific types of neuronal cells. Others claim that the rosettes are reminiscent of early neural tubes, and indeed they do express markers consistent with neural plate identity, such as Pax6, nestin, NCAM, and Sox1 [34].

In the current study, β-tubulin labeling in the APC reveals a scaffold associated with the rosettes as well as tethers between the rosettes. Microtubules of the eukaryotic cytoskeleton are composed of a heterodimer of α- and β-tubulin, each in itself a family of several highly homologous isoforms [35]. In vertebrates, six types of β-tubulin (class I to class VI) have been identified and these are thought to have functional and cell-type specificities [36]. For example, class III β-tubulin (also known as TuJ-1), one of the most specialized tubulins, is specific for neurons and committed neuronal precursors in birds and mammals, while there is evidence that class I β-tubulin is associated with neuronal commitment and adult neurogenesis in fish [36]. In mammals, the expression of the class III β-tubulin isotype has also been associated with rosette-type cells [37–39], suggesting that these cells are committed to a neural fate.

Among invertebrates, four β-tubulin isoforms have been identified in *Drosophila* [40,41], and three to five in crustaceans [42]. The *Drosophila* β3-tubulin gene has a structure extremely similar to that of the vertebrate β-tubulin genes [40]; however, the distribution patterns of the various isoforms have not linked a specific type with a neural fate [41].

The β-tubulin antibody used in the current experiments does not distinguish between different β-tubulin isotypes, and because so little is known about the distribution and function of various tubulins in crustacean tissues, defining the tubulin isotype will not clarify issues related to cellular commitment or fate. In the present study, therefore, β-tubulin labeling allowed an analysis and comparison of general morphological features of the posterior HPT and APC, but does not support functional conclusions. Nevertheless, the intriguing β-tubulin labeling associated with APC rosettes suggests a prominent role for these molecules in the organization of these assemblies of cells.

An antibody generated against tyrosinated tubulin also was used to label APC and posterior HPT. Tyrosination is a post-translational modification of the tubulin that leads to

the presence of tyrosinated tubulin at the dynamic plus-ends of microtubules, while older and more stable microtubules are mainly composed of detyrosinated tubulin (glutamylated-tubulin) [43,44]. Antibodies against tyrosinated tubulin have therefore been particularly useful in the developing nervous system where cytoskeletal reorganization is rampant and, indeed, these antibodies have been employed to reveal the crayfish neurogenic niche and streams as these emerge around the time of hatching [7]. In the current work, tyrosinated tubulin immunoreactivity is found in the cytoplasm of APC cells, perhaps reflecting the dynamic cytoskeletal rearrangements associated with the high degree of mitotic activity in which these cells are engaged. In contrast, tyrosinated tubulin in the posterior HPT is found in fibrous elements resembling those associated with the early proto-niche during development [7]. This labeling may suggest that these fibers, like the growth cone, are involved in dynamic shape changes or are active extensions of HPCs.

At this stage in our work, the significance of rosettes in the APC is not obvious. Nevertheless, the "bowl-shaped cell clusters" of Noonin et al. [9] that arise from APC cells in vitro are remarkably similar to the rosettes formed by cultured human embryonic stem cells (e.g., compare Fig. 10 in Ref. [9] and Fig. 4 in Ref. [13]), indeed suggesting that rosette formation in culture could be indicative of a multipotent stem cell type. The common feature in the many systems where rosettes have been identified is that these structures represent an early developmental stage that is generally associated with a neuroectodermal fate. A meaningful interpretation of the APC rosettes awaits immunocytochemical, molecular biological, and fate studies of these intriguing cell assemblies.

## Acknowledgments

The authors thank P. Carey and V. LePage for care of the animals used in these studies, and Melanie Prasol for critical comments on the article. The studies reviewed in this article were supported by NSF IOS 1121345 (to B.S.B.) and Brazilian Financial Agency CAPES (to P.G.C.S.).

## Author Disclosure Statement

No competing financial interests exist.

## References

1. Harzsch S and RR Dawirs. (1996). Neurogenesis in the developing crab brain: post-embryonic generation of neurons persists beyond metamorphosis. J Neurobiol 28:384–398.
2. Schmidt M and S Harzsch. (1999). Comparative analysis of neurogenesis in the central olfactory pathway of adult decapod crustaceans by *in vivo* BrdU labeling. Biol Bull 196:127–136.
3. Sullivan JM, JL Benton, DC Sandeman and BS Beltz. (2007a). Adult neurogenesis: a common strategy across diverse species. J Comp Neurol 500:574–584.
4. Sullivan JM, DC Sandeman, JL Benton and BS Beltz. (2007b). Adult neurogenesis and cell cycle regulation in the crustacean olfactory pathway: from glial precursors to differentiated neurons. J Mol Histol 38:527–542.
5. Zhang Y, S Allodi, DC Sandeman and BS Beltz. (2009). Adult neurogenesis in the crayfish brain: proliferation, migration and possible origin of precursor cells. Dev Neurobiol 69:415–436.
6. Benton JL, Y Zhang, CR Kirkhart, DC Sandeman and BS Beltz. (2011). Primary neuronal precursors in adult crayfish brain: replenishment from a non-neuronal source. BMC Neurosci 12:53.
7. Sintoni S, JL Benton, BS Beltz, BS Hansson and S Harzsch. (2012). Neurogenesis in the central olfactory pathway of adult decapod crustaceans: development of the neurogenic niche in the brains of Procambarid crayfish. Neural Dev 7:1.
8. Chaves da Silva PG, JL Benton, BS Beltz and S Allodi. (2012). Adult neurogenesis: ultrastructure of a neurogenic niche and neurovascular relationships. PLoS One 7:e39267.
9. Noonin C, X Lin, P Jiravanichpaisal, K Söderhäll and I Söderhäll. (2012). Invertebrate hematopoiesis: an anterior proliferation center as a link between the hematopoietic tissue and the brain. Stem Cells Dev 21:3173–3186.
10. Meshorer E and T Misteli. (2006). Chromatin in pluripotent embryonic stem cells and differentiation. Nat Rev Mol Cell Biol 7:540–546.
11. Owusu-Anash E and U Banerjee. (2009). Reactive oxygen species prime *Drosophila* haematopoietic progenitors for differentiation. Nature 46:537–541.
12. Ito K, A Hirao, F Arai, K Takubo, S Matsuoka, K Miyamoto, M Ohmura, K Naka, K Hosokawa, Y Ikeda and T Suda. (2006). Reactive oxygen species act through p38 MAPK to limit the lifespan of hematopoietic stem cells. Nat Med 12:446–451.
13. Wilson PG and SS Stice. (2006). Development and differentiation of neural rosettes derived from human embryonic stem cells. Stem Cell Rev 2:67–77.
14. Elkabetz Y, G Panagiotakos, G Al Shamy, ND Socci, V Tabar and L Studer. (2008). Human ES cell-derived neural rosettes reveal a functionally distinct early neural stem cell stage. Genes Dev 22:152–165.
15. Mirzadeh Z, FT Merkle, M Soriano-Novarro, JM Garcia-Verdugo and A Alvarez-Buylla. (2008). Neural stem cells confer unique pinwheel architecture to the ventricular surface in neurogenic regions of the adult brain. Cell Stem Cell 3:265–278.
16. Kuznetsov AV, I Kehrer, AV Kozlov, M Haller, H Redl, M Hermann, M Grimm and J Troppmair. (2011). Mitochondrial ROS production under cellular stress: comparison of different detection methods. Anal Bioanal Chem 400: 2383–2390.
17. Beltz BS, Y Zhang, JL Benton and DC Sandeman. (2011). Adult neurogenesis in the decapod crustacean brain: a hematopoietic connection? Eur J Neurosci 34:870–883.
18. Maynard DM. (1960). Circulation and heart function. In: *The Physiology of Crustacea.* Waterman TH, ed. Academic Press, New York, pp 162–226.
19. Steinacker A. (1978). The anatomy of the decapod crustacean auxiliary heart. Biol Bull 154:497–507.
20. Baumann H. (1917). Das core frontale bei decapoden Krebsen. Zool Anz 49:137–144.
21. Sandeman DC. (1967). The vascular circulation in the brain, optic lobes and thoracic ganglia of the crab *Carcinus*. Proc R Soc Lond B Biol Sci 168:82–90.
22. Bauchau AG. (1981). Crustaceans. In: *Invertebrate Blood Cells.* Ratcliffe NA, AF Rowley, eds. Academic Press, New York, pp 385–420.
23. Martin GG, JE Hose, M Choi, R Provost, G Omori, N McKrell and G Lam. (1993). Organization of hematopoietic

tissue in the intermolt lobster, *Homarus americanus*. J Morphol 216:65–78.
24. Chaga O, M Lignell and K Söderhäll. (1995). The hematopoietic cells of the freshwater crayfish, *Pacifastacus leniusculus*. Anim Biol 4:59–70.
25. Söderhäll I, E Bangyeekhun, S Mayo and K Söderhäll. (2003). Hemocyte production and maturation in an invertebrate animal; proliferation and gene expression in hematopoietic stem cells of *Pacifastacus leniusculus*. Dev Comp Immunol 27:661–672.
26. Söderhäll I, YA Kim, P Jiravanichpaisal, SY Leea and K Söderhäll. (2005). An ancient role for a prokineticin domain in invertebrate hematopoiesis. J Immunol 174:6153–6160.
27. Sullivan JM and BS Beltz. (2005). Newborn cells in the adult crayfish brain differentiate into distinct neuronal types. J Neurobiol 65:157–170.
28. Hammond J, D Cai and KJ Verhey. (2008). Tubulin modifications and their cellular functions. Curr Opin Cell Biol 20:71–76.
29. Lin X and I Söderhäll. (2011). Crustacean hematopoiesis and the astakine cytokines. Blood 117:6417–6424.
30. Ghiretti-Magaldi A, C Milanese and G Tognon. (1977). Hematopoiesis in crustaceans decapoda: origin and evolution of hemocytes and cyanocytes of *Carcinus maenus*. Cell Differ 6:167–186.
31. Lin X, M Novotny, K Söderhäll and I Söderhäll. (2010). Ancient cytokines—the role of astakines as hematopoietic growth factors. J Biol Chem 285:28577–28586.
32. Harris TJC and M Peifer. (2004). Adherens junction-dependent and -independent steps in the establishment of epithelial cell polarity in *Drosophila*. J Cell Biol 167:135–147.
33. Hava D, U Forster, M Matsuda, S Cui, BA Link, J Eichhorst, B Wiesner, A Chitnis and S Abdelilah-Seyfried. (2008). Apical membrane maturation and cellular rosette formation during morphogenesis of the zebrafish lateral line. J Cell Sci 122:687–695.
34. Germain N, E Banda and L Grabel. (2010). Embryonic stem cell neurogenesis and neural specification. J Cell Biochem 111:535–542.
35. Dutcher SK. (2001). The tubulin fraternity: alpha to eta. Curr Opin Cell Biol 13:49–54.
36. Oehlmann VD, S Berger, C Sterner and SI Korsching. (2004). Zebrafish beta tubulin 1 expression is limited to the nervous system throughout development, and in the adult brain is restricted to a subset of proliferative regions. Gene Expr Patterns 4:191–198.
37. Caccamo DV, MM Herman, A Frankfurter, CD Katsetos, VP Collins and LJ Rubinstein. (2009). An immunohistochemical study of neuropeptides and neuronal cytoskeletal proteins in the neuroepithelial component of a spontaneous murine ovarian teratoma. Primitive neuroepithelium displays immunoreactivity for neuropeptides and neuron-associated beta-tubulin isotype. Am J Pathol 1135:801–813.
38. Katsetos CD, MM Herman, A Frankfurter, S Uffer, E Perentes and LJ Rubinstein. (1991). Neuron-associated class III beta-tubulin isotype, microtubule-associated protein 2, and synaptophysin in human retinoblastomas *in situ*. Further immunohistochemical observations on the Flexner-Wintersteiner rosettes. Lab Invest 64:45–54.
39. Koch P, T Opitz, JA Steinbeck, J Ladewig and O Brüstle. (2009). A rosette-type, self-renewing human ES cell-derived neural stem cell with potential for *in vitro* instruction and synaptic integration. Proc Natl Acad Sci U S A 106:3225–3230.
40. Rudolph J, M Kimble, HD Hoyle, MA Subler and EC Raff. (1987). Three *Drosophila* beta-tubulin sequences: a developmentally regulated isoform (β3), the testis-specific isoform (β2), and an assembly-defective mutation of the testis-specific isoform ($B2t^8$) reveal both an ancient divergence in metazoan isotypes and structural constraints for beta-tubulin function. Mol Cell Biol 7:2231–2242.
41. Hoyle HD and EC Raff. (1990). Two *Drosophila* beta tubulin isoforms are not functionally equivalent. J Cell Biol 111: 1009–1026.
42. Demers DM, AE Metcalf, P Talbot and BC Hyman. (1996). Multiple lobster tubulin isoforms are encoded by a simple gene family. Gene 171:185–191.
43. Webster DR, GG Gundersen, JC Bulinski and GG Borisy. (1987). Differential turnover of tyrosinated and detyrosinated microtubules. Proc Natl Acad Sci U S A 84:9040–9044.
44. Paturle L, J Wehland, RL Margolis and D Job. (1989). Complete separation of tyrosinated, detyrosinated, and nontyrosinatable brain tubulin subpopulations using affinity chromatography. Biochemistry 28:2698–2704.

Address correspondence to:
*Dr. Barbara S. Beltz*
*Neuroscience Program*
*Wellesley College*
*106 Central Street*
*Wellesley, MA 02481*

*E-mail:* bbeltz@wellesley.edu

Received for publication October 17, 2012
Accepted after revision November 21, 2012
Prepublished on Liebert Instant Online November 26, 2012